

Supplementary Information

Exploiting oncogene-induced replicative stress for the selective killing of Myc-driven tumors

Matilde Murga^{1,6}, Stefano Campaner^{2,6}, Andres J. Lopez-Contreras¹, Luis. I. Toledo¹, Rebeca Soria¹, Maria F. Montaña¹, Luana D' Artista², Thomas Schleker², Carmen Guerra³, Elena Garcia⁴, Mariano Barbacid³, Manuel Hidalgo⁴, Bruno Amati^{2,5} and Oscar Fernandez-Capetillo¹

¹Genomic Instability Group, Spanish National Cancer Research Centre (CNIO), Madrid, Spain.

²Department of Experimental Oncology, European Institute of Oncology (IEO), at the IFOM-IEO Campus, Milan, Italy. ³Experimental Oncology Group, Spanish National Cancer Research Centre (CNIO), Madrid, Spain. ⁴Clinical Research Program, Spanish National Cancer Research Centre (CNIO), Madrid, Spain. ⁵Center for Genomic Science of IIT@SEMM, Istituto Italiano di Tecnologia (IIT), at the IFOM-IEO Campus, Milan, Italy. ⁶These authors contributed equally to this work. Correspondence should be addressed to M.M. (mmurga@cnio.es) or O.F.-C. (ofernandez@cnio.es).

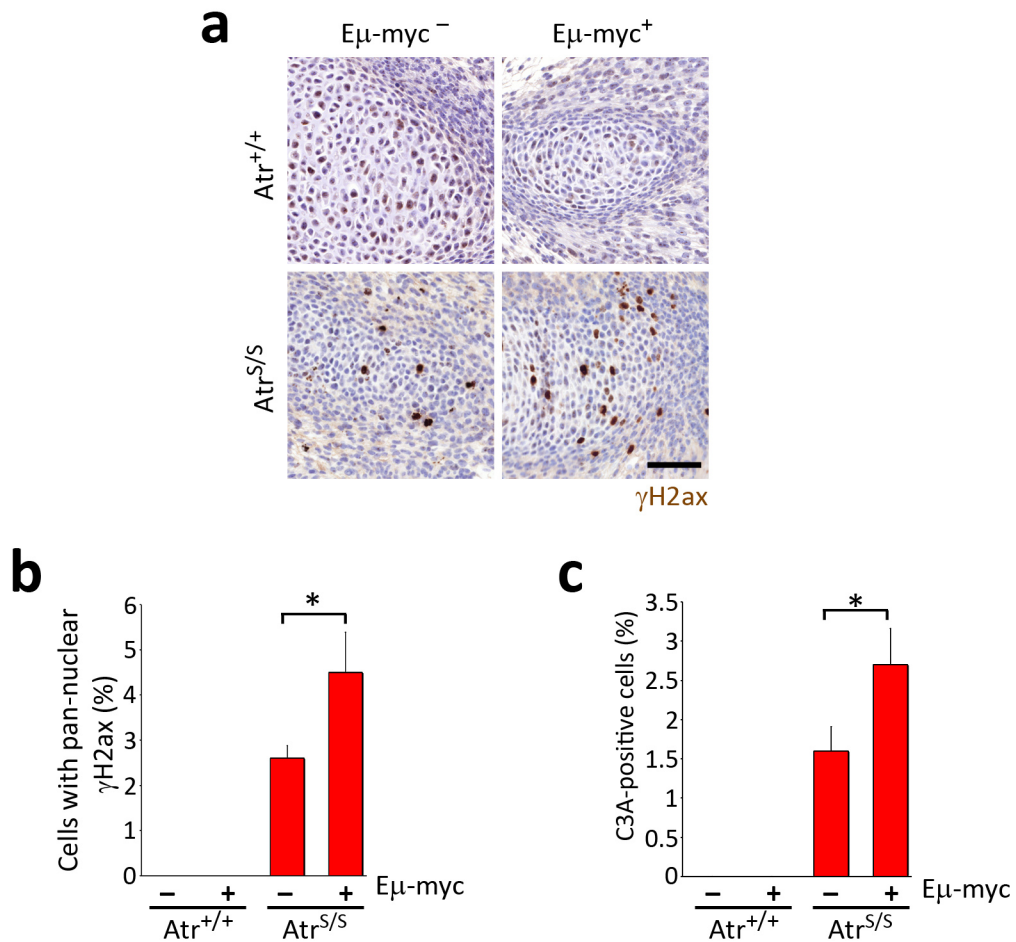


Fig. S1 $E\mu\text{-myc}$ increases the abundance of embryonic DNA damage and apoptosis on *Atr*-Seckel mice. **(a)** Immunohistochemistry (IHC) of γH2ax on the developing bone of 13.5 dpc embryos of the indicated genotypes. Scale bar indicates 50 μm . **(b)** Quantification from **(a)**. **(c)** Quantification of activated caspase-3 IHC positive cells in embryos of the indicated phenotypes. (n=4, *: $P < 0.05$)

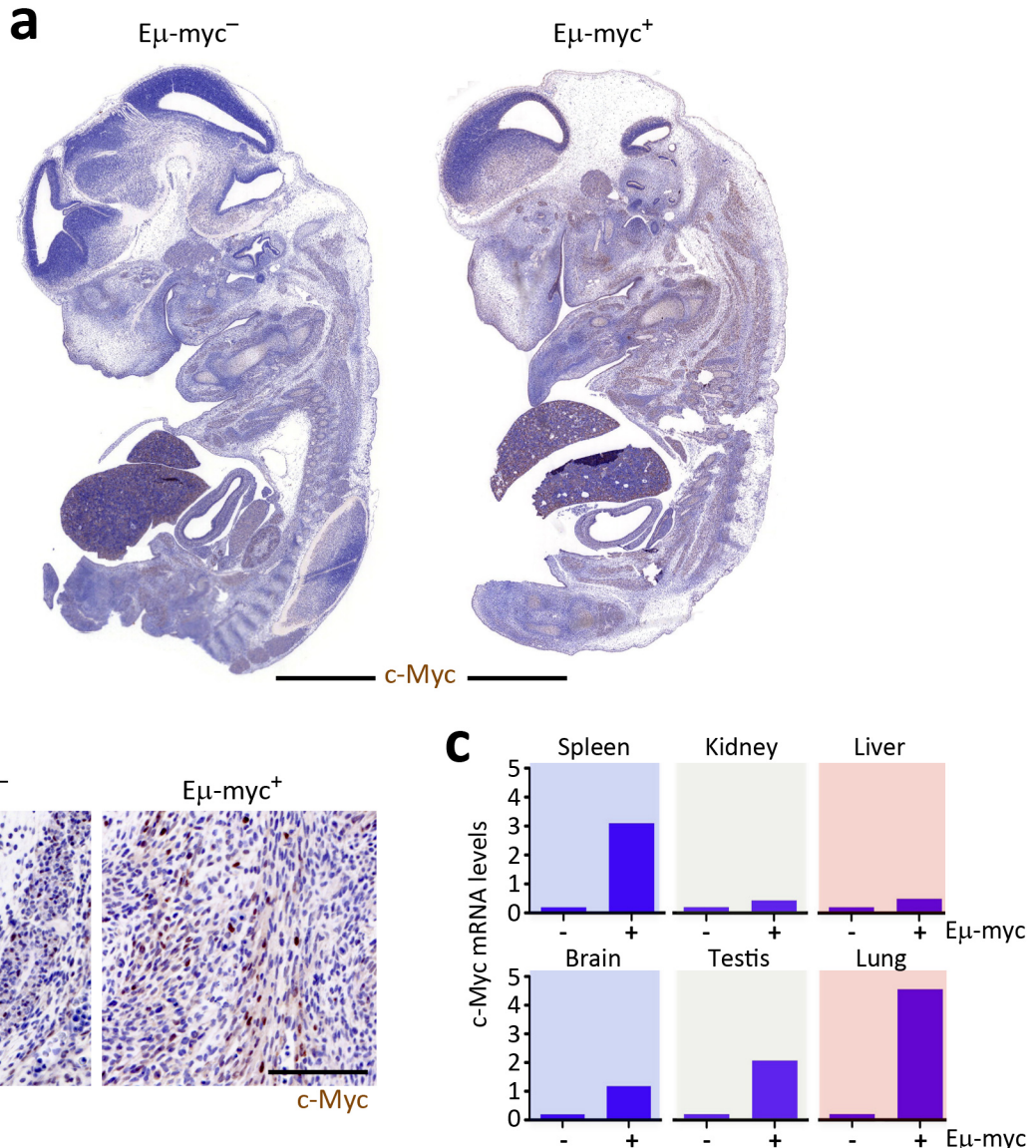


Fig. S2 Increased levels of c-Myc on $E\mu\text{-myc}^+$ mice and embryos. **(a)** c-Myc IHC on sagittal sections of 13.5 dpc littermate embryos of the indicated genotypes. **(b)** Close-up of an embryonic section of the analysis described in **(a)**. Black scale bar indicates 100 μm . **(c)** qRT-PCR mediated analysis of c-Myc mRNA levels in the indicated tissues of 2 month old $E\mu\text{-myc}^-$ and $E\mu\text{-myc}^+$ mice. Levels of GADPH were used to normalize for total mRNA levels.

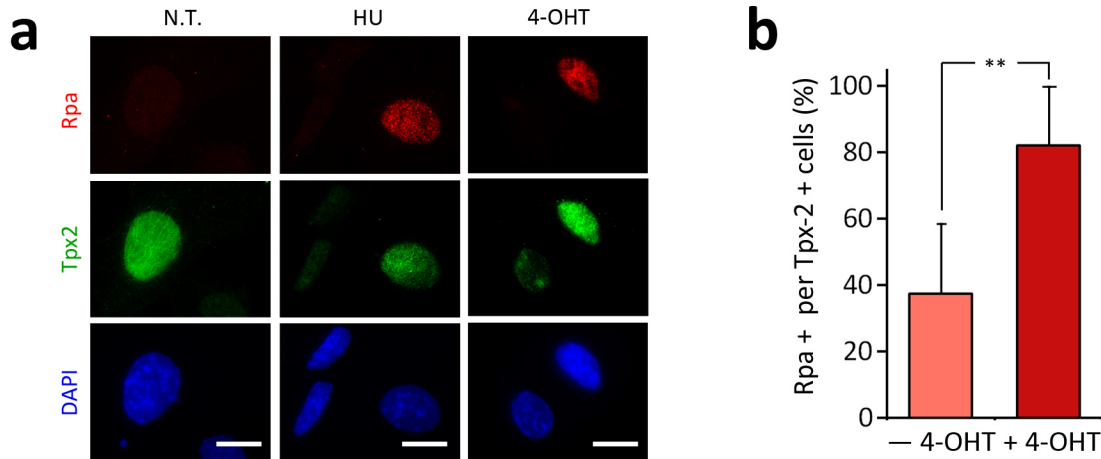


Fig. S3 MycER activation induces Rpa foci in S/G2 cells. **(a)** The images illustrate the staining pattern of Rpa (red) that can be obtained by immunofluorescence in MEF that have been untreated, treated with the replicative stress-inducing agent hydroxyurea (HU, 2mM-3hr) or infected with MycER and treated with 4-OHT for 24 hrs. The staining was done following a pre-extraction protocol that removes the nucleoplasmic fraction of proteins. Tpx2 was used as an extraction-resistant marker of S/G2 cells. Scale bar (white) indicates 5 μ m. **(b)** Quantification of the percentage of Tpx-2 positive cells showing Rpa foci. (**: $P < 0.01$).

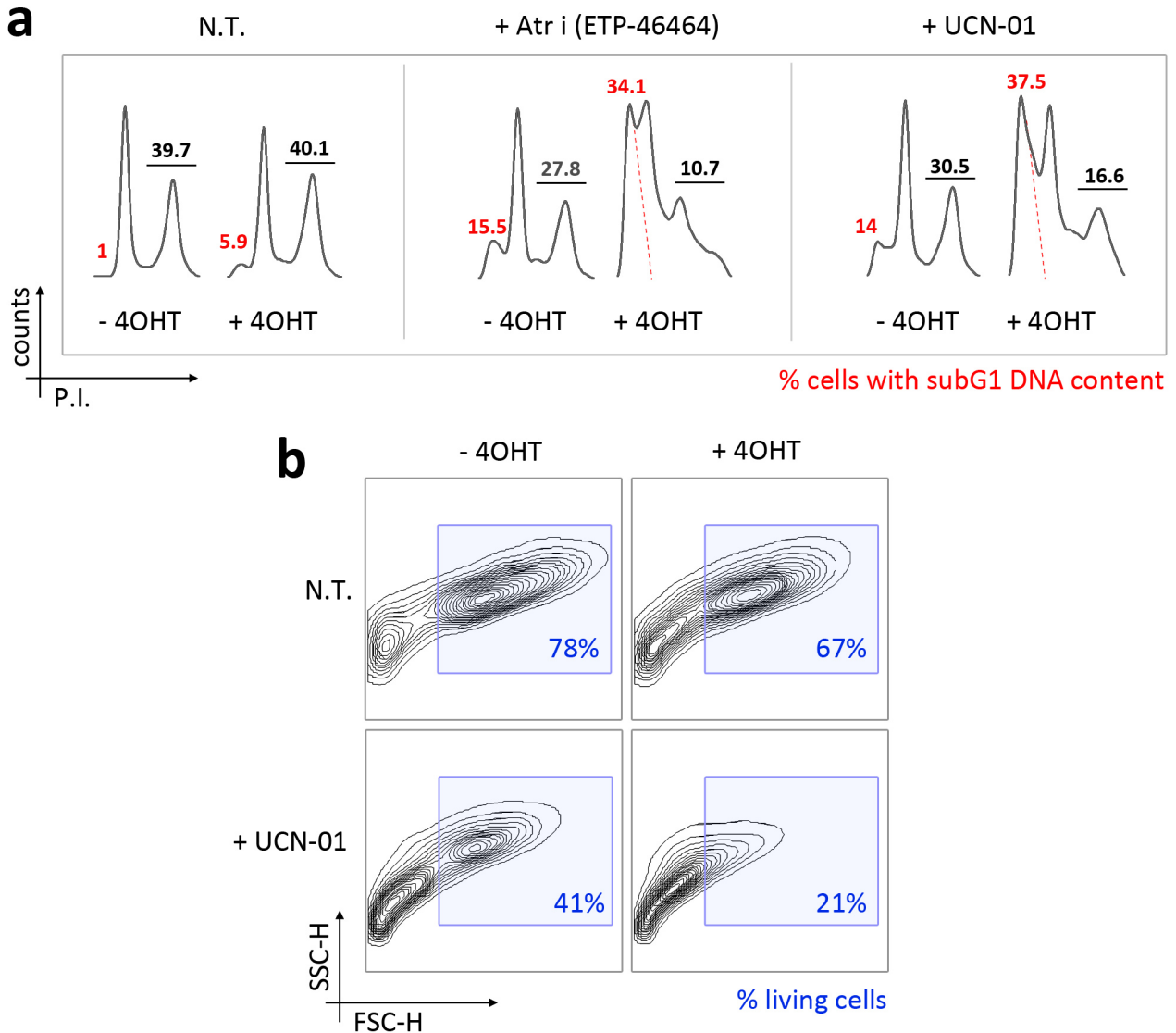


Fig. S4 Atr and Chk1 inhibitors sensitize cells for Myc-induced apoptosis. **(a)** Cell cycle profiles of MycER infected MEF in the presence or absence of 4-OHT and/or an Atr inhibitor¹ (ETP-46464, 5 μ M) or Chk1 inhibitor (UCN-01, 300 nM) for 48 hrs. Sub-G1 (red) and S/G2 (black) percentages are indicated. **(b)** The panels show the number of living cells that remain in the cell cultures analyzed in **(a)**, and it is used to illustrate that the actual toxicity of this strategy is higher than that indicated by the subG1 analysis (which is done by previously gating on “live” cells on the flow cytometer).

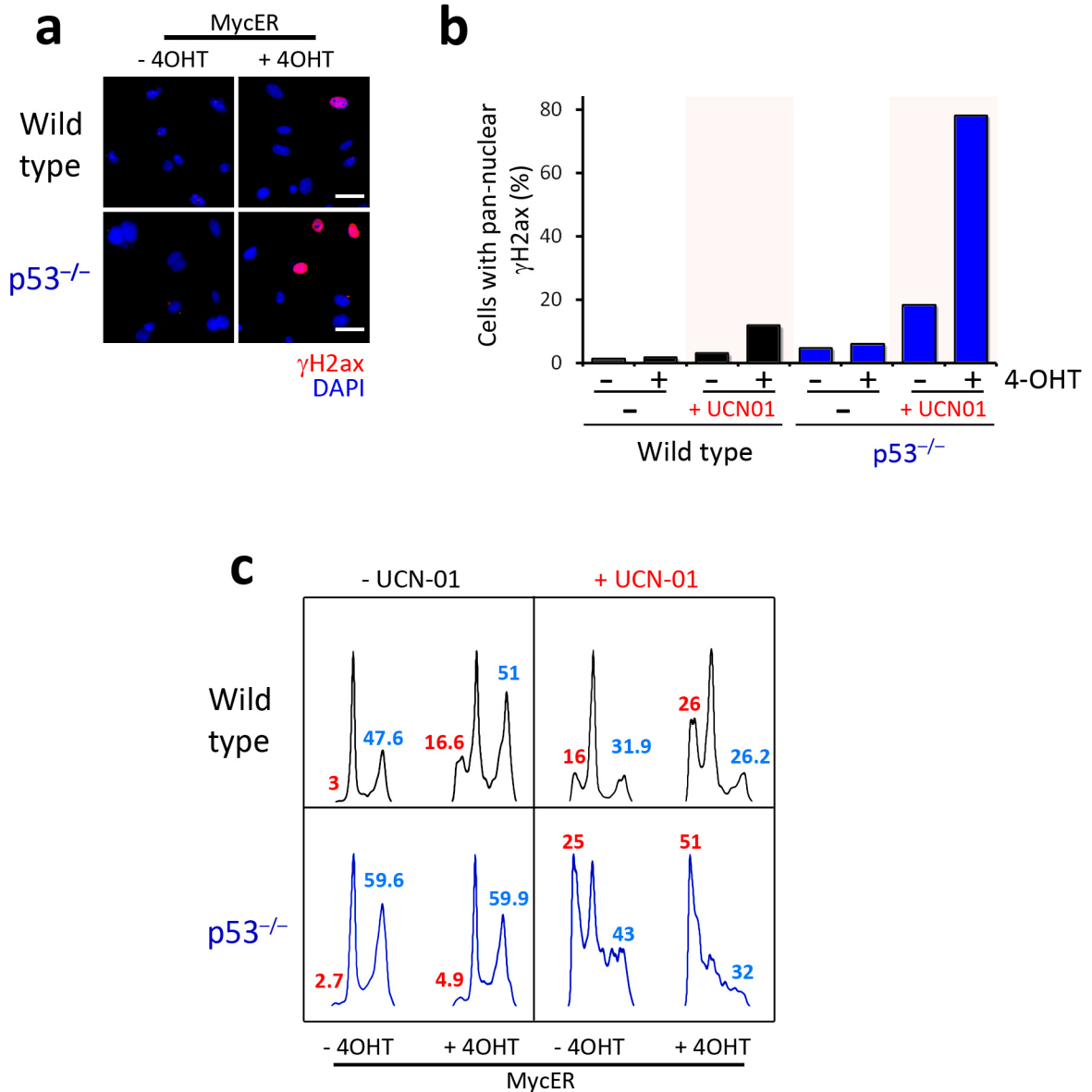


Fig. S5 Myc-induced apoptosis in p53-deficient MEF. **(a)** Images illustrating the staining pattern of the γ H2ax (red) signal on wt and p53^{-/-} MycER-infected MEF, treated or untreated with 4-OHT for 24 hrs. Scale bar indicates 10 μ m. **(b)** Percentage of cells showing a pan-nuclear distribution of γ H2ax in wt and p53^{-/-} MycER-infected MEF, treated or untreated with 4-OHT for 24 hrs, and in the presence or absence of UCN-01 (300 nM). **(c)** Cell cycle profiles of MycER infected MEF of the different genotypes in the presence or absence of 4-OHT for 48 hrs. Sub-G1 (red) and S/G2 (blue) percentages are indicated. The data show a representative experiment that was repeated 3 times with independent MEF pairs.

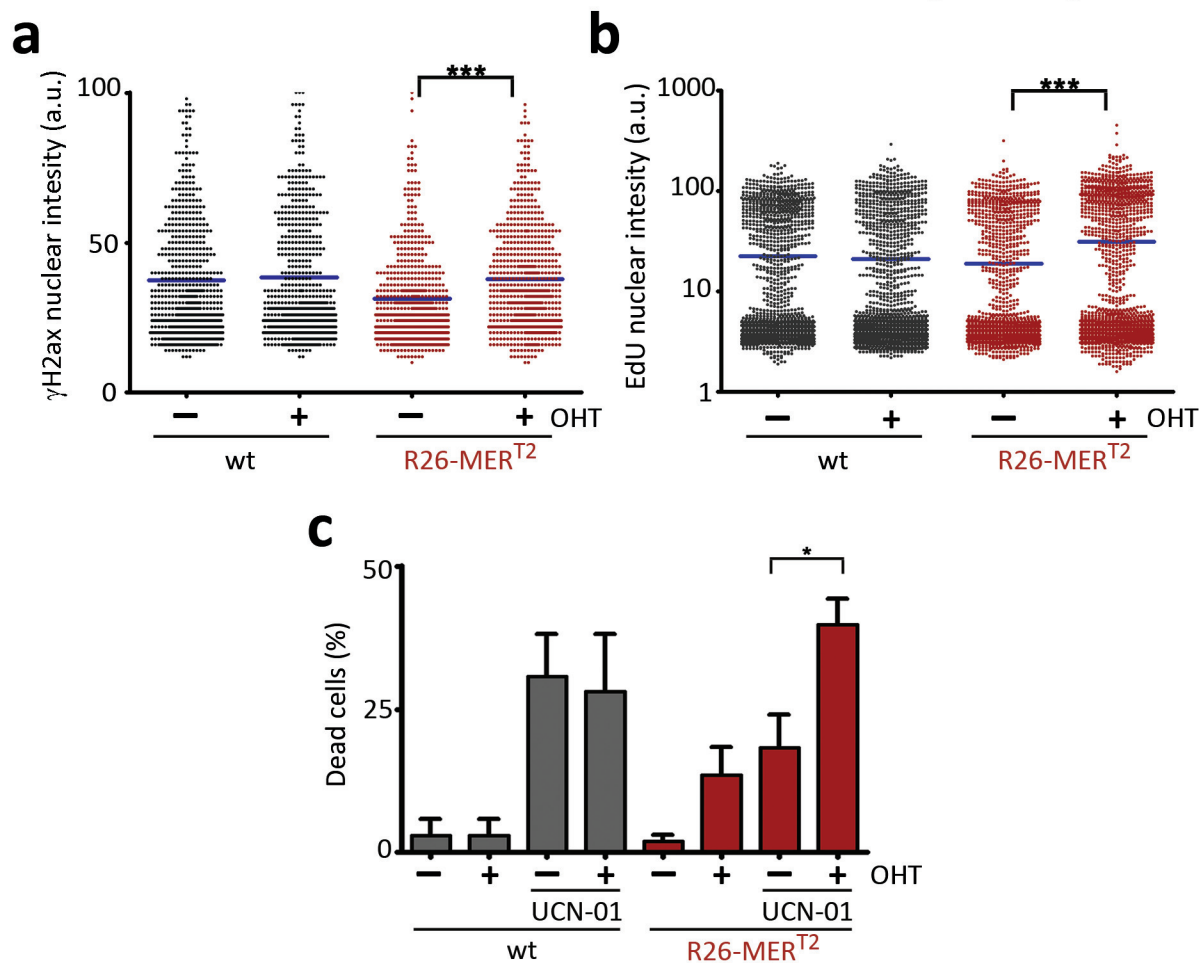


Fig. S6 Myc-induced RS in R26MER^{T2} MEF. R26MER^{T2} MEF derive from a strain in which the MycER^{T2} construct was knocked-in at the ROSA26 locus². **(a)** Activation of Myc in these MEF with 4-OHT for 24 hrs led to an increase in replicative stress (as measured with the nuclear γ H2ax signal). **(b)** Similarly, 4-OHT promoted higher rates of DNA replication on R26MER^{T2} MEF (as measured with EdU). EdU was given for the last h after a 24 h exposure to 4-OHT). **(c)** The % of dead cells (quantified as in Figs. S4,5) is shown for wt and R26MER^{T2} MEF after a 48 h treatment with 4-OHT and/or UCN-01 (300 nM). Panels **(a)** and **(b)** were obtained through High Throughput Microscopy analyses of γ H2AX and EdU signals, respectively (as explained in³). The presence of replicative stress in R26MER^{T2} MEF is consistent with the fact that these MEF present a p53-response when exposed to 4-OHT (Evan, G.I.; personal communication).

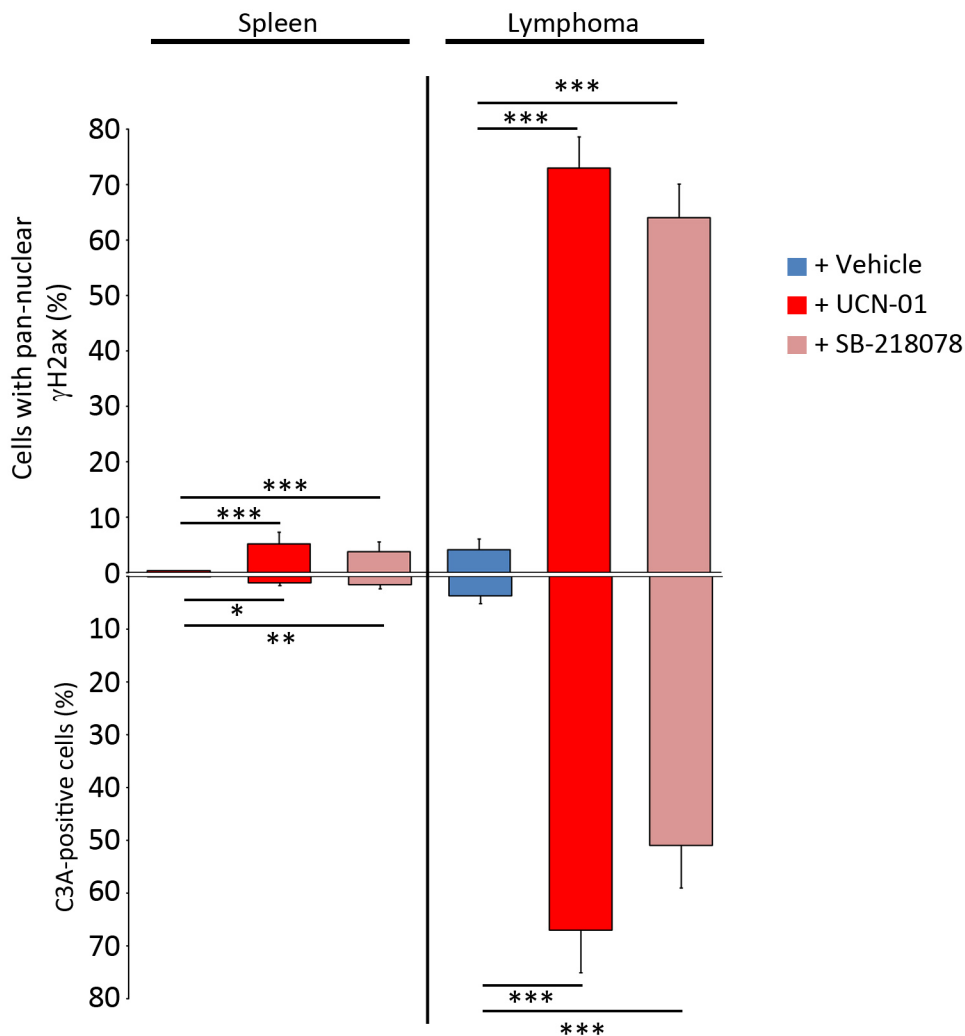


Fig. S7 Effect of a single injection of Chk1 inhibitors in Myc-induced lymphomas. Quantification of the percentages of cells presenting a pan-nuclear staining of γ H2ax or activated caspase-3 (C3A) on the spleens of mice with or without Myc-induced lymphomas, after a 16 hr treatment with UCN-01 or SB-218078 (5 mg per kg) (n=5; *: $P < 0.05$; **: $P < 0.01$; ***: $P < 0.001$).

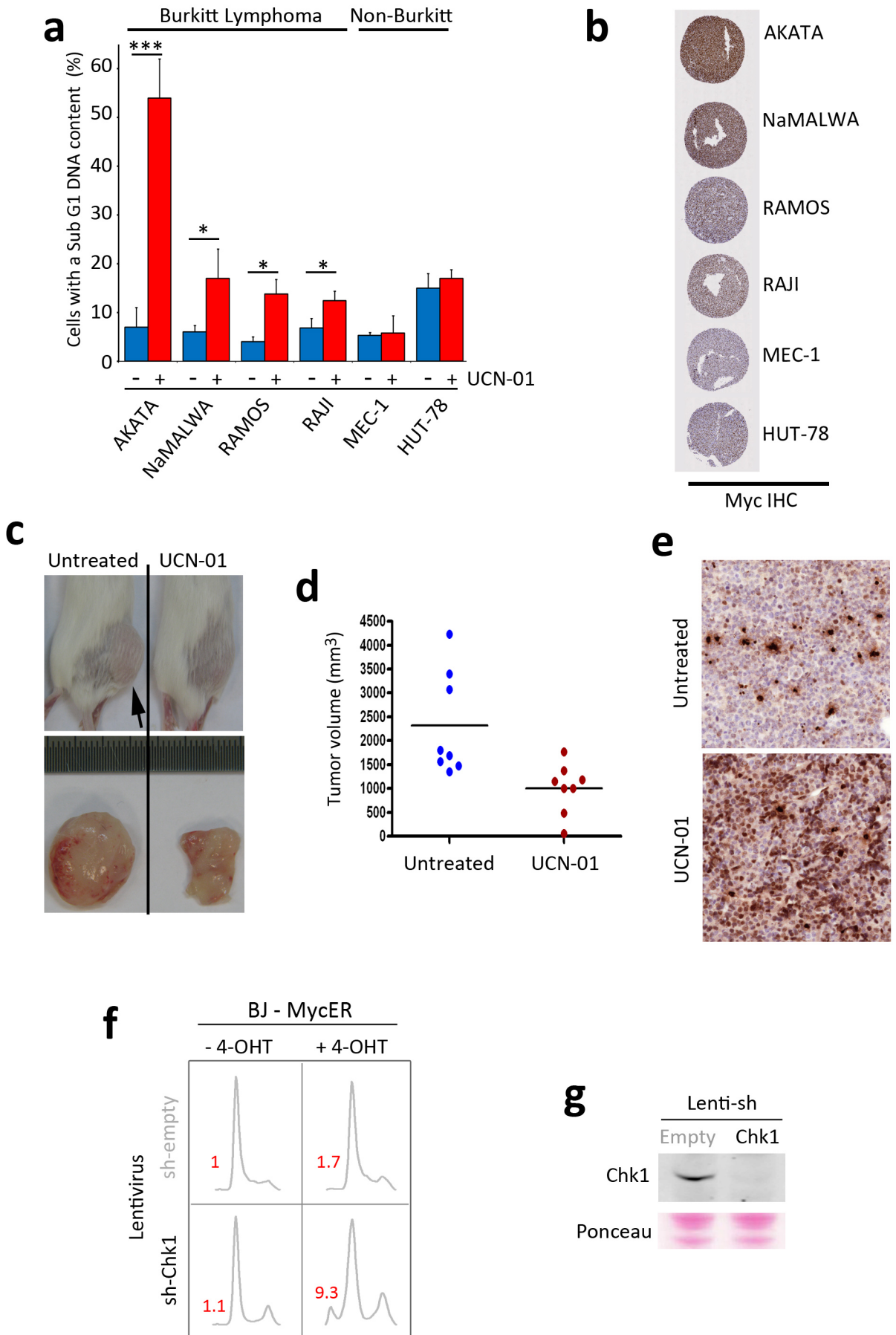


Fig. S8 Synthetic lethality between Myc and Chk1 in human cells. **(a)** Percentages of subG1 cells of several human cell lines in response to UCN-01 (300nM, 24 h). The drug is particularly toxic for Burkitt-lymphoma lines which are associated with Myc translocations and amplifications. (n=3; *: $P < 0.05$; ***: $P < 0.001$). **(b)** c-Myc levels in the different cell lines analyzed. Note that the sensitivity of Chk1 inhibitors is particularly notorious in the Burkitt lines presenting the highest levels of Myc. **(c)** Representative pictures of SCID mice carrying subcutaneous xenografts of NaMALWA human Burkitt lymphoma cells, after being treated for 9 days with UCN-01 (5 mg per kg). For the generation of the xenografts, 5 million cells were subcutaneously injected in cold PBS. Tumors became visible after 2-3 weeks. **(d)** Tumor volumes of the xenografts mentioned in **(c)** after a 9 day treatment with UCN-01 ($P = 0.0159$). **(e)** Representative pictures of the γ H2ax IHC from NaMALWA xenografts, 16 h after a treatment with UCN-01 (vs untreated). **(f)** Cell cycle profiles of MycER infected BJ-hTERT cells, which had been simultaneously infected with Chk1-targeting shRNA expressing lentiviruses (or control lentiviruses), in the presence or absence of 4-OHT and for 48 h. Sub-G1 (red) percentages are indicated. The data show a representative experiment that was repeated 3 times with independent infections. Note that BJ cells are less sensitive to MycER-induced apoptosis than MEF or B lymphocytes, which probably reflects the lower replication rates present in these cells. **(g)** Western blot illustrating the depletion of Chk1 upon lentiviral infection with the shRNA expressing virus.

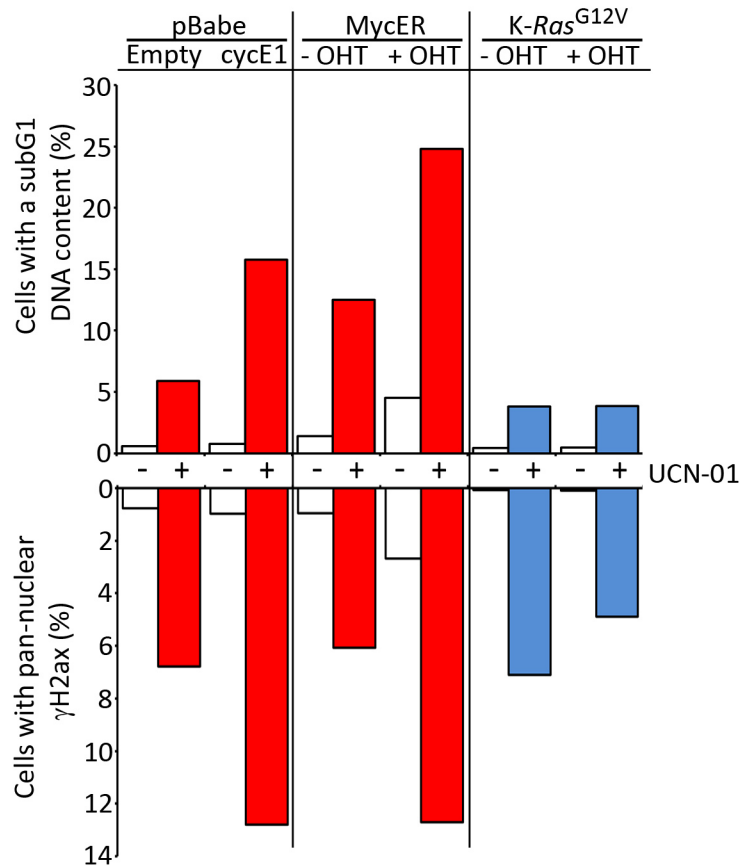


Fig. S9 Differential effects of Chk1 inhibition on Ras, cyclin E1 and Myc oncogenes. Quantification of the percentages of cells (MEF) presenting a pan-nuclear γ H2ax staining or subG1 DNA content in the presence or absence of UCN-01. The conditions for the different oncogenes were: (1) Cyclin E1 (cycE1): Cells were infected with a cycE1 expressing retrovirus (pBabe-puro-cycE1) or control vector (pBabe-puro), selected in puromycin for 3 days and then treated or untreated with UCN-01 for 48 h. (2) Myc: MycER infected cells were selected in puromycin for three days and then treated or untreated with UCN-01 for 48 h in the presence or absence of 4-OHT. (3) Ras: MEF carrying an oncogenic allele of *K-Ras*^{G12V} that is conditionally induced upon Cre-mediated recombination⁴, and a CreER^{T2} allele which induces Cre-mediated cleavage in the presence of 4-OHT, were treated with 4-OHT for 7 days to promote the expression of the oncogenic allele in every cell (which was verified with a β -Geo marker; data not shown). UCN-01 was then added for 48 h. The graph illustrates the data from one representative experiment that was conducted in parallel for all oncogenes. We have recently reported the same synthetic lethal effect of Atr inhibitors on cycE1 overexpressing cells, which occurs independently of p53¹.

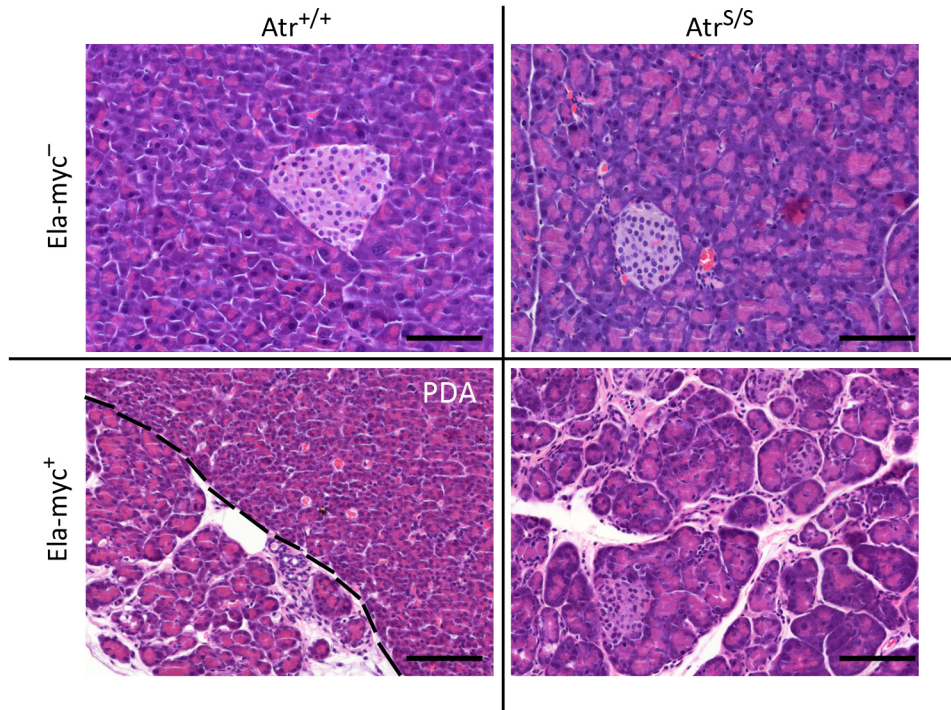


Fig. S10 Reduced *Atr* levels abrogate pancreatic ductal adenocarcinomas induced by *Myc*. Top panels illustrate the overall architecture of the pancreas, which is conserved in *Atr*-Seckel mice. The left bottom panel shows one example of the pancreatic ductal adenocarcinomas (PDA) that are found on *Ela-myc* mice at 16 weeks of age (the tumoral area is separated by black dashed lines). PDA are normally found as distinct lobules, made up of disorganized and crowded regions of acinar cells that are devoid of islets of langerhans. Whereas the presence of *Ela-myc* led to a disorganized and dysplastic pancreas both on *Atr*^{+/+} and *Atr*^{S/S} mice, no PDAs were ever found on *Atr*-Seckel mice. Scale bar (black), indicates 100 μm.

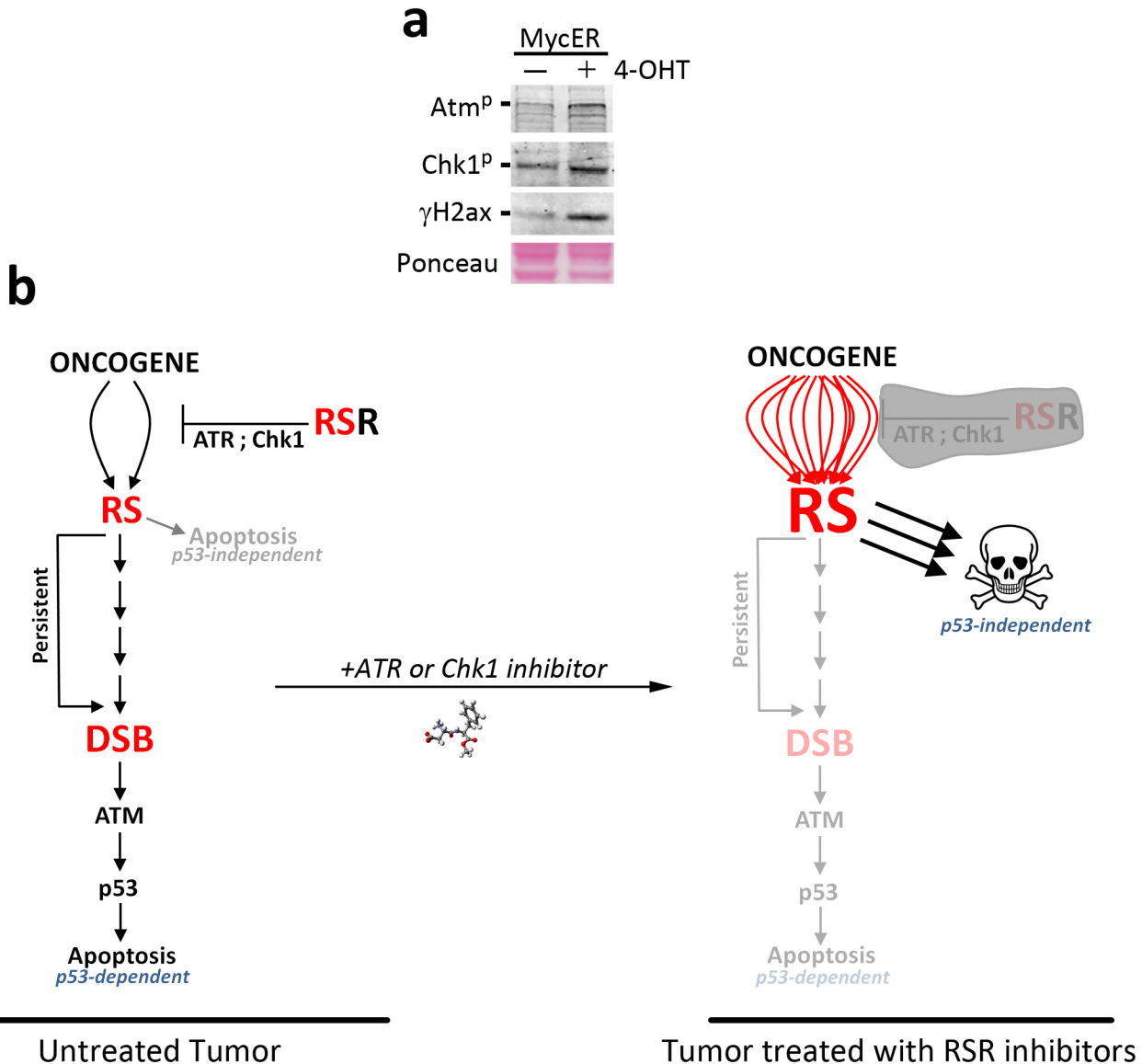


Fig. S11 Targeting Atr or Chk1 for cancer treatment. **(a)** Western blot from MycER infected MEF in the presence or absence of 4-OHT for 48 h that illustrates, as previously shown for Myc-induced lymphomas⁵, the concomitant presence of an activated Atm- and Atr-dependent response. **(b)** The figure provides a refined view of the oncogene-induced DNA damage model⁶ that illustrates the coexistence of p53 dependent and independent apoptotic pathways that are induced by oncogenes. Oncogenes would generate small amounts of replicative stress, which, *per se*, might not be significantly apoptotic. However, persistent replicative stress would ultimately lead to the generation of DSB, which would activate the canonical ATM-p53-apoptotic DDR. Hence, a replicative stress/p53-independent and a DSB/p53-dependent and apoptotic pathway would coexist in certain tumors. In these cases, a treatment with Atr or Chk1 inhibitors would exacerbate the amounts of replicative stress induced by oncogenes, unleashing a potent p53-independent apoptotic response. In summary, targeting Atr or Chk1 would be synthetic lethal for tumors with high levels of replicative stress, providing a rationale for the use of these drugs in cancer chemotherapy.

Supplementary References

1. Toledo, L.I., *et al.* A cell-based screen identifies ATR inhibitors with synthetic lethal properties for cancer-associated mutations. *Nat Struct Mol Biol* **18**, 721-727 (2011).
2. Murphy, D.J., *et al.* Distinct thresholds govern Myc's biological output in vivo. *Cancer Cell* **14**, 447-457 (2008).
3. Guerra, C., *et al.* Tumor induction by an endogenous K-ras oncogene is highly dependent on cellular context. *Cancer Cell* **4**, 111-120 (2003).
4. Gorrini, C., *et al.* Tip60 is a haplo-insufficient tumour suppressor required for an oncogene-induced DNA damage response. *Nature* **448**, 1063-1067 (2007).
5. Halazonetis, T.D., Gorgoulis, V.G. & Bartek, J. An oncogene-induced DNA damage model for cancer development. *Science* **319**, 1352-1355 (2008).